ChemPhysChem

Chemistry Europe
European Chemical Societies Publishing

Accepted Article

Title: Enhancement of Negative Photochromic Properties of Naphthalene-Bridged Phenoxyl-Imidazolyl Radical Complex

Authors: Jiro Abe, Hiroki Ito, and Katsuya Mutoh

To be cited as: *ChemPhysChem* 10.1002/cphc.202000296

Link to VoR: https://doi.org/10.1002/cphc.202000296

WILEY-VCH

10.1002/cphc.202000296

WILEY-VCH

ARTICLE

Enhancement of Negative Photochromic Properties of Naphthalene-Bridged Phenoxyl-Imidazolyl Radical Complex

Hiroki Ito[a], Katsuya Mutoh[a] and Jiro Abe*[a]

[a] H, Ito, Dr. K. Mutoh, Prof. J. Abe*
Department of Chemistry
School of Science and Engineering, Aoyama Gakuin University
5-10-1 Fuchinobe, Chuo-ku, Sagamihara, Kanagawa 252-5258, Japan
E-mail: jiro_abe@chem.aoyama.ac.jp

Supporting information for this article is given via a link at the end of the document.

Abstract: Negative photochromism has increased attention as a light-switch for functional materials. A development of fast photochromic molecules has been also expected because a rapid thermal back reaction within a millisecond time scale is useful for real-time switching. Herein, we synthesized the derivatives of the naphthalene-bridged phenoxyl-imidazolyl radical complex (Np-PIC) showing the negative photochromism to demonstrate the efficient strategy to increase the visible light sensitivity and to control the thermal back reaction rates. The distances of the C–C bond of the transient 2,4'-isomer shows good agreement with the thermodynamic stability, leading to the control of the thermal back reaction rate. We revealed the cyclic voltammetry and the DFT calculations are efficient to predict the characters of the HOMO and LUMO. The introduction of the electron-withdrawing dicyanoquinodimethane group is efficient to induce the photochromic reaction with increased visible-light sensitivity by the expansion of the π-conjugation. The results will give an important insight for the future development of fast-responsive negative photochromic molecules.

Introduction

Photochromic molecules are one of the important photoswitches not only to control the color, but also to switch electronic and magnetic properties, mechanical works, and biological activities.[1–4] Though almost common photochromic molecules respond to UV light in at least one way of the reversible photoswitching reactions, increasing the visible light sensitivity has been recently considered to avoid unexpected reactions and degradations by harmful UV light. In addition, the excitation UV light cannot penetrate into the inside of the photochormic materials because the colored species re-absorbs the excitation light on the surface.

Negative photochromism, in which a thermally stable colored isomer photoisomerizes to a transient colorless isomer upon visible light irradiation, has increased much attention as a novel photoswitch.[5–14] A negative photochromic reaction has some advantages over a conventional positive photochromic reaction: photosensitivity to energetically low toxic visible light and deep penetration of excitation light inside materials. Although several novel negative photochromic molecules have been reported, the slow thermal back reaction in minutes and the strong dependence on the solvent polarity limit the application and capability of negative photochromic molecules. Because the switching ability within milliseconds is attractive for a real-time control for photochromic lenses,[15,16] fluorescence property,[17,18] holographic materials,[19,20] a development of fast-switchable negative photochromic molecules will be important to open a new area of photochromism. Recently, we developed negative photochromic binaphthyl-bridged imidazole dimer (BN-ImD) derivatives which show decoloration reaction upon visible light irradiation.[21–24] Because the thermal back reaction of BN-ImD does not depend on the solvent polarity, BN-ImD will be able to work as a photoswitch in various mediums. The thermal back reaction can be accelerated to the second time scale by replacing one of the imidazole rings to the phenoxyl ring.[25] The naphthalene-bridged phenoxyl-imidazolyl radical complex (Np-PIC, **1**) also shows the fast thermal back reaction in the millisecond time scale.[26] However, the efficient strategy to control the photosensitivity and the thermal back reaction rate has not been explored yet. Therefore, in this study, we investigated the photochromic properties of Np-PIC derivatives to reveal the relationship between the electronic structures and the photochromic properties. We designed the Np-PIC derivatives (Scheme 1), **2** in which an imidazole and a phenoxyl units are bridged by 1,2-dihydroacenaphthylene, **3** in which a phenoxyl unit of Np-PIC is replaced by a dicyanoquinodimethane unit, **4** in which an imidazole and a phenoxyl units are bridged by acenaphthylene, **5** in which an imidazole and a dicyanoquinodimethane units are bridged by an acenaphthylene unit, and **6** in which the π-conjugation of the imidazole unit is extended by a pyreno-imidazole unit.

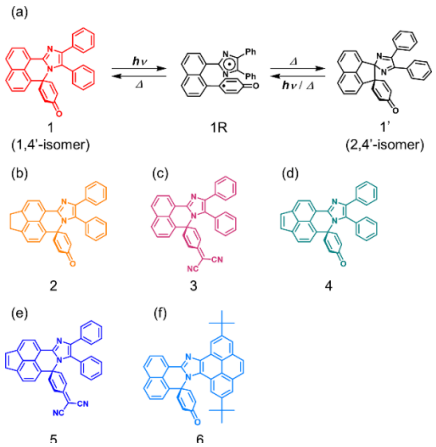

Scheme 1. (a) The scheme of the negative photochromic reaction of Np-PIC (**1**). (b–f) The molecular structures of the Np-PIC derivatives in this study.

Results and Discussion

UV–vis Absorption Spectroscopy

The molecular structures of **2**–**6** were revealed unambiguously by the X-ray crystallographic analyses of the single crystals (Figure 1). The all derivatives are the 1,4'-isomers that is the most thermally stable structural isomer. The imidazole ring and the electron accepter units (the phenoxyl or the dicyanoquinodimethane unit) of the all derivatives are perpendicularly oriented as same as that of **1**. The distances of the C–N bond are almost similar with that of **1** (ca. 1.49 Å).[26]

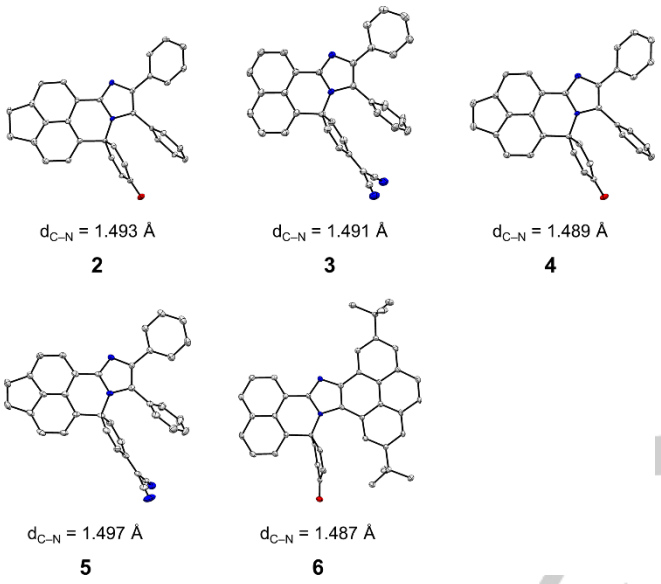

Figure 1. ORTEP representations of the molecular structures of **2–6** with thermal ellipsoids (50 % probability), where the nitrogen atoms are highlighted in blue and the oxygen atom is highlighted in red. The hydrogen atoms are omitted.

The UV–vis absorption spectra of **1**–**6** in benzene are shown in Figure 2a. Figure 3 shows the energy levels of the molecular orbitals calculated by the DFT calculations (MPW1PW91/6-31+G(d)//MPW1PW91/6-31G(d)). Compound **1** has the absorption band at around 370 nm which is attributable to the transition from the orbital delocalized over the bridging naphthalene and the imidazole units (HOMO) to the π*-orbital on the naphthalene unit.[26] Compound **2** shows the similar absorption spectrum with that of **1** because the single-bond bridge of the 1,2-dihydroacenaphthylene unit does not affect the π-conjugation of the naphthalene unit, that is consistent with the results of the DFT calculations. Compound **3** has a small absorption band at 450 nm in addition to the absorption band at 370 nm. The absorption band at 450 nm of **3** is attributable to the HOMO−2 to the LUMO transition (Figure S31). The TDDFT calculation revealed that the $S_1 \leftarrow S_0$ transition of Np-PIC is assigned to the HOMO → LUMO transition. However, the transition probability is almost zero due to the small overlap integral between the perpendicularly oriented HOMO and LUMO. Thus, the reduction of the energy level of the π* orbital is efficient to increase the photosensitivity to visible light. In contrast to the 1,2-dihydroacenaphthylene bridge, the acenaphthylene bridge effectively expands the π-conjugation, leading to the decrease in the energy level of the π* orbital. In fact, **4** and **5** have intense absorption bands reached to 550 nm in the visible light region as shown in Figure 2. The TDDFT calculations of **4** and **5** indicate these absorption bands can be assigned to the HOMO → LUMO and the HOMO → LUMO+1 transitions, respectively (Figure 3). The expansion of the π-conjugation of the naphthalene unit largely decreases the energy level of the π*-orbital, lowering the photo-excitation energy. Therefore, the double-bond bridge for the naphthalene unit effectively extends the π-conjugation and to enhance the visible light sensitivity. The pyreno-imidazole unit is also efficient to increase the visible light sensitivity because of the planar structure as shown in Figure 1. The absorption band at around 420 nm can be assigned to the charge transfer (CT) transition from the electron-donating pyrenyl unit to the electron-withdrawing naphthalene unit (HOMO → LUMO+1).

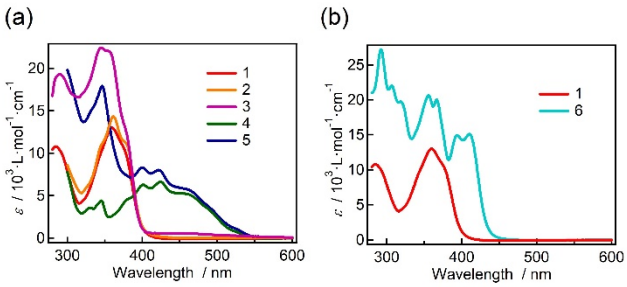

Figure 2. UV-vis absorption spectra of **1**–**6** in benzene at 298 K.

DFT calculation for the Np-PIC derivatives

The femtosecond time-resolved absorption spectroscopy and the electrochemical measurement of the photochromic imidazole dimer and the phenoxyl-imidazolyl radical complex derivatives have revealed that the C–N bond breaking reaction proceeds from the S_1 state to generate the biradical species because the LUMO has the anti-bonding character in relation to the C–N bond (C–N*).[27–30] The 1,4'-isomer of Np-PIC is also expected that the biradical species which thermally isomerizes to the 2,4'-isomer is generated upon UV light irradiation.[26] As shown in Figure 3, the LUMOs of **1**, **2** and **6** are similar to that of the typical PIC derivative having the anti-bonding character in relation to the C–N bond. However, it is presumed that **4** does not show the photochromic reaction from the S_1 state because the energy level of the π*-orbital is lower than that of the C–N* orbital. The introduction of the electron-accepter group to the phenoxyl unit of Np-PIC will be efficient to reduce the energy level of the C–N* orbital because the C–N* orbital is localized on the phenoxyl unit. The dicyanomethylene group has known as a strong electron-withdrawing group and it is easy to substitute a carbonyl group with a dicyanomethylene group. The energy level of the C–N* orbital of **3** is largely decreased by the introduction of a dicyanomethylene group with small change in the energy level of the π*-orbital. Based on the theoretical calculations, we expected **5** would show the photochromic reaction with enhanced visible-

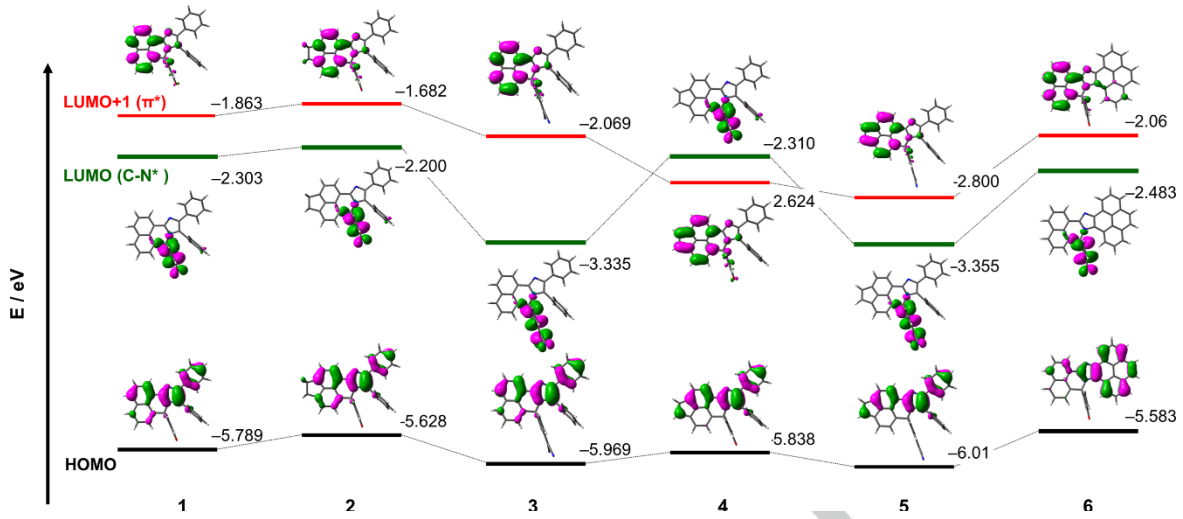

Figure 3. The relevant molecular orbitals of **1**–**6** (MPW1PW91/6-31+G(d)//MPW1PW91/6-31G(d)).

light photosensitivity because of the significantly reduced energy level of the C–N* orbital lower than the π*-orbital.

Cyclic Voltammetry

The cyclic voltammetry (CV) is one of the efficient methods to predict the HOMO and LUMO levels of molecules. It has been revealed by the detail investigations of the CV measurement of imidazole dimer and PIC derivatives that an electron injection to the LUMO leads to the generation of the radical anion species in which the C–N bond spontaneously breaks to form the radical and the anion species (the ECE process as shown in Scheme 2).[29–31] The subsequent reduction of the generated radical species to generate the dianion species is simultaneously proceeded at the same reduction potential of the initial dimer. Figure 4 shows the cyclic voltammograms of the Np-PIC derivatives. The cyclic voltammograms are similar to those of the previously reported PIC derivatives. Thus, it can be considered that Np-PIC derivatives show the same electrochemical reaction with those of the PIC derivatives. Table 1 summarizes the reduction and oxidation peaks and the estimated energy gaps between the HOMO and LUMO of **1**−**6**. The HOMO–LUMO gaps were approximately estimated by using the redox peaks due to the irreversibility. The irreversible reduction peaks of the 1,4'-isomers **1**, **2**, **4** and **6** were observed at −1.37–−1.58 V, which can be assigned to the ECE process to produce the dianion species. The reduction peaks of **3** and **5** are shifted to more positive potentials (−0.85 and −0.81 V, respectively) by introducing the electron-withdrawing dicyanomethylene group. These results are consistent with the DFT calculations (Figure 3). The electrochemical oxidation of **1**–**6** would produce the radical cation species as similar with the oxidation of the PIC derivatives.[32] The oxidation potential of **6** is shifted to more negative potential, compared with those of **1**–**5** because of the electron-donating ability of the pyrenyl unit. The order of the HOMO−LUMO gaps calculated by the DFT calculations (MPW1PW91/6-31+G(d)//MPW1PW91/6-31G(d)) is in good agreement with that estimated by the CV measurements.

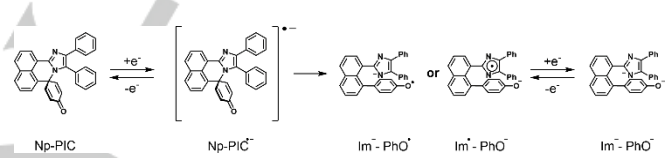

Scheme 2. The redox behaviour of Np-PIC.

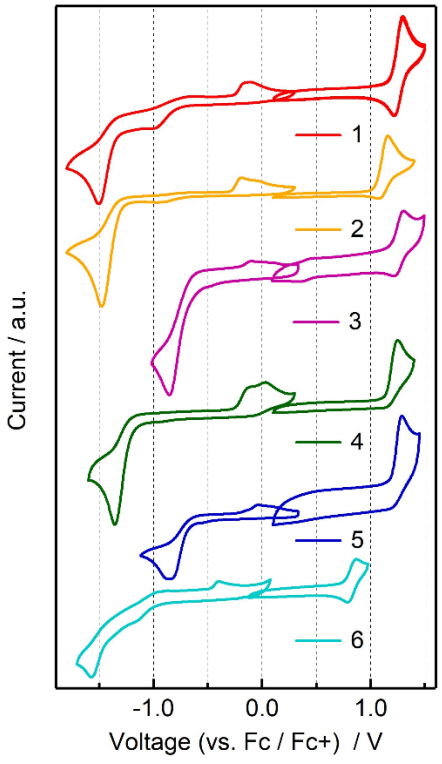

Figure 4. Cyclic voltammograms of **1** (red line), **2** (orange line), **3** (purple line), **4** (green line), **5** (blue line), **6** (light blue line) in CH_2Cl_2 (1.0 mM) containing 0.1 M (TBA)PF_6 as a supporting electrolyte. Potential scan rate = 500 mV/s.

Table 1. Electrochemical Reduction ($E_{red.}$), Oxidation ($E_{ox.}$) Peaks, and the HOMO−LUMO Gaps ($E_{g,exp}$) Estimated by Electrochemistry and the Excitation Energies ($E_{ex.}$) Estimated by TDDFT Calculations (MPW1PW91/6-31+G(d)// MPW1PW91/6- 31G(d))

compounds	$E_{red.}$ (V)	$E_{ox.}$ (V)	$E_{g,exp}$ (eV)	$E_{ex.}$ (eV)
1	−1.51	1.30	2.81	2.80
2	−1.48	1.16	2.64	2.63
3	−0.85	1.30	2.15	2.07
4	−1.37	1.24	2.61	2.56
5	−0.81	1.28	2.09	2.00
6	−1.58	0.87	2.45	2.37

Time-Resolved Absorption Spectroscopy

Figure 5 shows the time-resolved absorption spectra and the temporal changes of the transient absorbance of **2**, **3** and **6** measured by laser flash photolysis exciting with a 355-nm nanosecond laser pulse. The negative bleaching signals were observed upon UV light irradiation. On the other hand, **4** and **5** did not show such negative absorption changes from the picosecond to the second time region. The reason on this point will be discussed in detail later. The bleach signals of **2**, **3** and **6** monotonically recovered to the initial absorption spectra with the half-lives of 5.8 μs, 0.26 ms and 5.8 ms at 298 K, respectively, in the whole spectral region. The spectral shapes of the bleach signals are similar with the absorption spectra of the initial thermally stable 1,4'-isomers. It is suggested from the similarity of the spectral change with that of **1** that the negative photochromic reaction from the 1,4'-isomer to the 2,4'-isomer is observed upon UV light irradiation.[26] Although the generation of the short-lived biradical species was suggested in the previous study of **1**, we could not observe clear absorption spectra of the biradical in a few hundreds of picosecond time region due to the degradation of the compounds during the accumulation of the time-resolved absorption spectra.

The thermal back reaction rate of **2** is much accelerated by bridging with a 1,2-dihydroacenaphthylene unit, compared with those of the other derivatives. It is known as the linear free-energy relationship that the change in the Gibbs free energy ($\Delta\Delta G_0$) between the initial state and the thermally metastable state is proportional to the change in the activation energy barrier ($\Delta\Delta G^{\ddagger}$) between the transition state and the thermally metastable state.[33] Table 2 summarizes the ΔG_0 values calculated by the DFT (MPW1PW91/6-31G(d)) between the 2,4'-isomer and the 1,4'-isomer, and the calculated bond distances of the C–C bond (d_{c-c}) between the 2-position of the imidazole ring and 4'-position of the phenoxyl or the dicyanoquinodimethane unit of 2,4'-isomer. The large ΔG_0 value of **2** leads to the acceleration of the thermal back reaction of the 2,4'-isomer. Because the magnitude relation of d_{c-c} and the ΔG_0 values show similar tendency, the increment of the d_{c-c} largely contributes to the destabilization of the 2,4'-isomer. The bridge of the C–C in 1,2-dihydroacenaphthylene or the C=C bond in acenaphthylene increases the distance between the 1- and 8-positions of the naphthalene unit due to the large steric distortion. This distortion of the naphthalene bridge hinders the formation of the five-membered ring of the 2,4'-isomer, resulting in the acceleration of the thermal back reaction of **2**. The plausible reason why the negative photochromism of **5** could not be observed would be due to the destabilization of the 2,4'-isomer by the C=C bond as discussed in the next section.

Table 2. The C–C Bond Distances of 2,4'-isomers of **1**–**6** and the ΔG_0 between the 1,4'-isomer and the 2,4'-isomer Calculated by the DFT (MPW1PW91/6-31G(d) level of the theory)

	1	**2**	**3**	**4**	**5**	**6**
d_{c-c} (Å)	1.610	1.633	1.613	1.636	1.641	1.611
ΔG_0 (kJ/mol)	84.1	112.7	77.8	117.5	113.4	85.2

Although the negative photochromic reactions of **4** and **5** were not observed from nanosecond to second time scales, the positive transient absorption bands were observed upon UV light irradiation to **4** and **5** in the picosecond and nanosecond time scale, respectively (Figure 6). The time-resolved absorption spectroscopic measuments of **4** and **5** were carried out by the time-resolved absorption spectroscopy from picosecond to nanosecond time scales by using the randomly interleaved pulse train (RIPT) method (Unisoku, picoTAS).[34] Since the LUMO of **4** is localized on the acenaphthylene unit (Figure 3), the photoirradiation to **4** does not promote the C–N bond breaking reaction based on Kasha's rule. The fluorescence lifetime of **4** was estimated to be 0.26 ns in benzene at 298 K. This is consistent with the lifetime estimated from the time-resolved absorption spectroscopy (0.29 ns). That is, the transient absorption spectrum of **4** can be assigned to the excited singlet state, and therefore **4** does not show the photochromic reaction. In contrast, the broad absorption band from 400 nm to 1000 nm with a lifetime of 100 ns was observed by the irradiation to **5** at 298 K. The fluorescence lifetime of **5** is much faster than the lifetime of the transient absorption spectrum, indicating that **5** generates a transient species upon UV light irradiation. The most plausible assignment of the transient species is the biradical generated by the C–N bond breaking reaction because the TDDFT calculation result of the biradical of **5** is in good agreement with the transient absorption spectrum (Figure S35). The stabilization of the biradical by the delocalization over the dicyanoquinodimethane unit would be the reason for the deceleration of the lifetime. There are two relaxation pathways after the generation of the biradical species, (i) the thermal back reaction to the initial 1,4'-isomer and (ii) the isomerization to the thermally unstable 2,4'-isomer. However, the biradical of **5** would not isomerize to the 2,4'-isomer because we could not observe the negative photochromic reaction. It can be considered that the destabilization of the 2,4'-isomer by bridging the naphthalene unit with a C=C bond also increases the activation energy barrier from the biradical to the 2,4'-isomer.

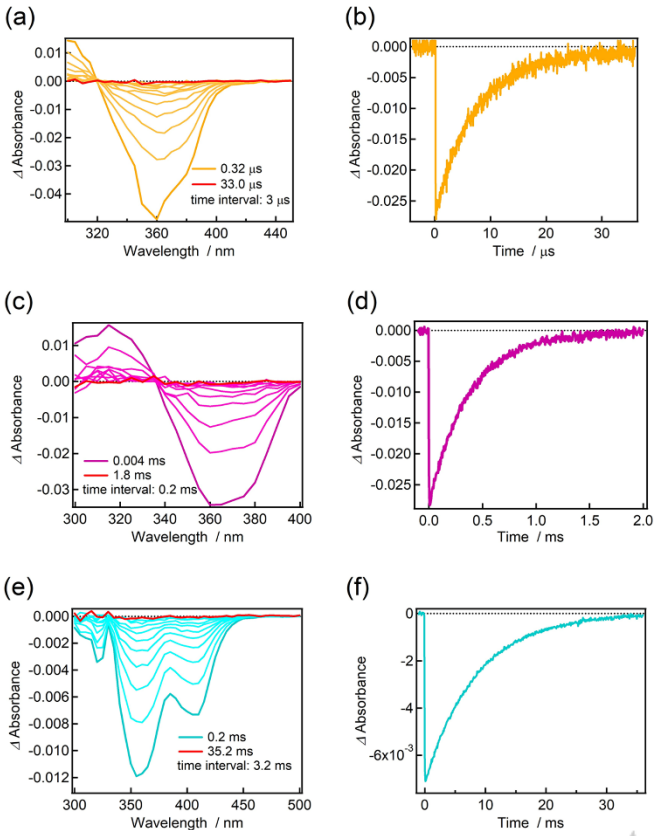

Figure 5. Transient absorption spectra and the time profiles of the transient absorbance of (a,b) **2**, (c, d) **3** and (e, f) **6** upon 355-nm nanosecond laser pulse irradiation (4 mJ) at 298 K in benzene (**2**: 2.6×10^{-5} M, **3**: 1.4×10^{-5} M, **6**: 1.7×10^{-5} M).

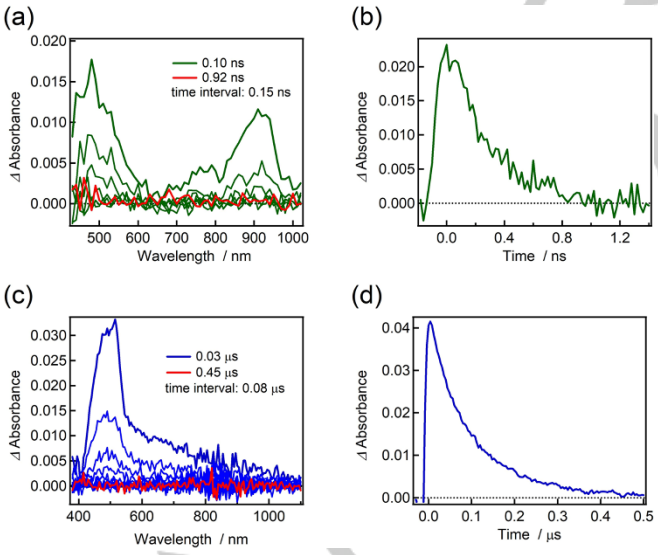

Figure 6. (a, b) Transient absorption spectra and the time profiles of the transient absorbance at 500 nm of **4** (1.7×10^{-4} M, in benzene) upon 355-nm picosecond laser pulse irradiation (1 kHz, 8 mW) at 298 K. (c, d) Transient absorption spectra and the time profiles of the transient absorbance at 500 nm of **5** (2.7×10^{-5} M, in benzene) upon 355-nm nanosecond laser pulse irradiation (4 mJ) at 298 K.

Conclusion

We investigated the strategy to improve the photochromic properties of the Np-PIC system by the combination of the DFT calculation, electrochemistry and time-resolved absorption spectroscopy. The extension of the π-conjugation of the imidazole unit is efficient to increase the visible light sensitivity. The bridge of an acenaphthylene unit instead of the naphthalene unit or the introduction of polycyclic aromatic hydrocarbon to the imidazole unit is suitable for Np-PIC derivatives. However, the replacement of a dicyanomethylene group to the phenoxyl group of Np-PIC is required to induce the photochromic reaction for the acenaphthylene-bridged PIC system by decreasing the energy level of the C–N* orbital possessing the anti-bonding character of the C–N bond. The thermal back reaction from the colorless 2,4'-isomer to the initial 1,4'-isomer can be accelerated by destabilizing the 2,4'-isomer with a 1,2-dihydroacenaphthylene bridge. The destabilization energy depends on the distance of the C–C bond between the imidazole and the phenoxyl units of Np-PIC. These insights will be important for the future development of fast switchable negative photochromic molecules.

Experimental Section

Voltammetry Measurements.

All cyclic voltammetry (CV) measurements were performed in a conventional three-electrode cell. A glassy carbon electrode (0.6 cm in diameter) was employed as a working electrode after polishing with 1 μm diamond on a diamond polishing pad and then with 0.05 μm alumina on an alumina polishing pad attached to a glass plate (ALS Co., Ltd.). The electrode was rinsed with pure acetone and dried in air before use. A platinum wire was used as a counter electrode, and an Ag/Ag+ reference electrode (Ag wire, 1 mM $AgNO_3$, 0.1 M tetrabutylammonium hexafluorophosphate in acetonitrile) was employed. All CV measurements were achieved from 0.05 to 1 V/s in solutions of 0.1 M (TBA)PF_6 in acetonitrile or dichloromethane at room temperature. Prior to each experiment, the solutions were deoxygenated by bubbling with nitrogen, and the nitrogen atmosphere was maintained throughout the course of the experiments. All potentials are referenced to the reversible formal potential for the ferrocene/ferrocenium (Fc/Fc^+) couple. μAutolab III potentiostat/ galvanostat (Metrohm Autolab B. V.) under computer control (General Purpose Electrochemical System software) was used for the CV measurement.

Time-Resolved Absorption Spectroscopy

The time-resolved absorption spectroscopy on microsecond to millisecond time scale was carried out with a TSP-2000 time-resolved spectrophotometer (Unisoku). A 10 Hz Q-switched Nd:YAG (Continuum Minilite II) laser with the third harmonic at 355 nm (5 ns pulse) was employed for the excitation light. A halogen lamp (OSRAM HLX64623) was used as a probe beam arranged in an orientation perpendicular to the exciting laser beam. The probe beam was monitored with a photomultiplier tube (Hamamatsu R2949) through a spectrometer (Unisoku MD200) for the decay profile of the colored species. The excitation intensity of one pulse was estimated by an energy monitor (Gentec Electro-Optics MAESTRO). Optical-grade solvents were used for all measurements. The measurements were performed in a benzene solution placed in a 1-cm quartz cell at 298 K. The time-resolved absorption spectroscopy on picosecond to nanosecond time scale was conducted by the randomly interleaved pulse train (RIPT) method.[34] A picosecond laser, PL2210A (EKSPLA, 1 kHz, 25 ps, 8 mW for 355 nm), and a supercontinuum (SC) radiation source (SC-450, Fianium, 20 MHz, pulse width: 50–100 ps depending on the wavelength, 450–2000 nm) were employed as the pump-pulse and probe sources, respectively. The measurements were

performed in a benzene solution placed in a 2-mm quartz cell under stirring at room temperature.

Synthesis.

All reactions were monitored by thin-layer chromatography carried out on 0.2 mm E. Merck silica gel plates (60F-254). Column chromatography was performed on silica gel (Silica gel 60N, Kanto Chemical). ^{1}H NMR and ^{13}C NMR spectra were recorded at 400 MHz on a Bruker AVANCE III 400 NanoBay. DMSO-d_6 and $CDCl_3$ were used as deuterated solvent. All glassware was washed with distilled water and dried. Unless otherwise noted, all reagents and reaction solvents were purchased from TCI, Wako Co. Ltd., Aldrich Chemical Co., Inc. and Kanto Chemical Co., Inc. and were used without further purification.

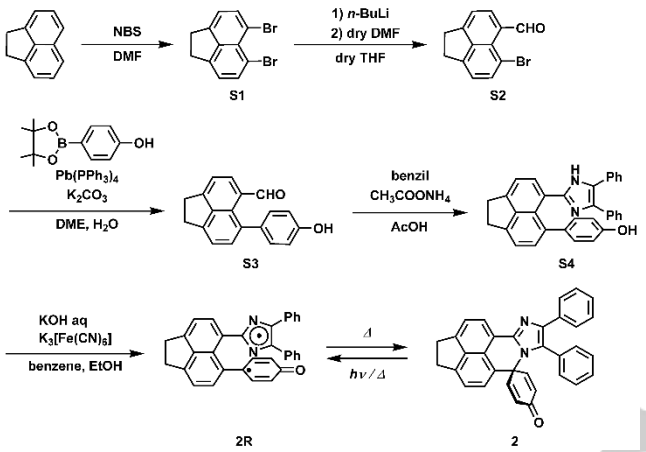

Scheme 3. Synthetic Scheme of **2**.

*5,6-Dibromo-1,2-dihydroacenaphthylene (**S1**)* was prepared according to a literature procedure.[35]

*6-Bromo-1,2-dihydroacenaphthylene-5-carbaldehyde (**S2**).* 1.50 mL (2.32 mmol) of *n*-butyl lithium solution (1.55 M in hexane) was added into a solution of 600 mg (1.93 mmol) of 5,6-dibromoacenaphthylene in 6 mL of anhydrous THF at −78 °C under N_2 atmosphere. The resulting reaction mixture was stirred at −78 °C for 20 minutes, treated with 1.2 mL (15.4 mmol) of anhydrous DMF, and then kept stirred at −78 °C for 30 minutes. The reaction mixture was slowly warmed to room temperature, and stirred for 30 minutes at room temperature. After the quenching with water, the reaction mixture was extracted with CH_2Cl_2. The organic extract was washed with water and brine, and filtered through a phase separator paper. After removal of the solvents, the crude product was purified by silica gel column chromatography (CH_2Cl_2/hexane = 2/1), to give desired product as a white solid (438.4 g, 86 %). ^{1}H NMR (400 MHz, $CDCl_3$) δ: 11.65 (s, 1H), 8.14 (d, *J* = 7.2 Hz, 1H), 7.87 (d, *J* = 7.2 Hz, 1H), 7.41 (d, *J* = 7.2 Hz, 1H), 7.23 (d, *J* = 7.6 Hz, 1H), 3.45-7.21 (m, 4H).

*6-(4-Hydroxyphenyl)-1,2-dihydroacenaphthylene-5-carbaldehyde (**S3**).* K_2CO_3 (147 mg, 1.06 mmol), 6-bromo-1,2-dihydroacenaphthylene-5-carbaldehyde (**S2**) (400 mg, 1.54 mmol), and 4-(4,4,5,5-tetramethyl-1,3,2-dioxaborolan-2-yl)phenol (400 mg, 1.85 mmol) were added to DME (7.2 mL) and water (4.0 mL) and the mixture was purged with N_2 gas. $Pd(PPh_3)_4$ (50 mg, 0.0432 mmol) was added to the solution and the solution was refluxed for 11 hours. The reaction mixture was extracted with CH_2Cl_2, and the organic extract was washed with water and brine, and filtered through a phase separator paper. After removal of the solvents, the crude product was purified by silica gel column chromatography (hexane/AcOEt = 5/1), to give desired product as a yellow solid (292 mg, 69 %). ^{1}H NMR (400 MHz, $CDCl_3$) δ: 9.65 (s, 1H), 8.08 (d, *J* = 7.2 Hz, 1H), 7.47 (d, *J* = 7.2 Hz, 1H), 7.41–7.37 (m, 2H), 7.32–7.30 (m, 2H), 6.93–6.91 (m,2H), 5.11 (s,1H), 3.47 (s,4H).

*4-(6-(4,5-Diphenyl-1H-imidazol-2-yl)-1,2-dihydroacenaphthylen-5-yl)phenol (**S4**).* 6-(4-hydroxyphenyl)-1,2-dihydroacenaphthylene-5-carbaldehyde (**S3**) (280 mg, 1.02 mmol), benzil (404 mg, 1.92 mmol) and ammonium acetate (985 mg, 12.8 mmol) were dissolved in acetic acid 13.6 mL. The mixture was stirred at 110 °C for 24 hours. After cooling to room temperature, the reaction mixture was neutralized with aqueous NH_3, and the aqueous layer was extracted with AcOEt. The combined organic layer was washed with water and brine, filtered through a phase separator paper. and evaporated. After removal of the solvents, the crude product was purified by silica gel column chromatography (hexane/AcOEt = 1/1), to give desired product as a yellow solid (233 mg, 50 %). ^{1}H NMR (400 MHz, DMSO-d_6) δ: 11.58 (s, 1H), 9.01 (s, 1H), 7.67 (d, *J* = 6.8 Hz, H), 7.45–7.14 (m, 12H), 6.92 (d, *J* = 7.2 Hz, 2H), 6.40 (d, *J* = 8.0 Hz, 2H), 3.45 (s, 4H).

*Compound **2**.* To a solution of 4-(6-(4,5-diphenyl-1*H*-imidazol-2-yl)-1,2-dihydroacenaphthylen-5-yl)phenol (**S4**) (200 mg, 0.430 mmol) in benzene 13 mL and ethanol 1.5 mL was added KOH (2.04 g, 35.6 mmol) and $K_3[Fe(CN)_6]$ (1.54 g, 4.56 mmol) in water 13 mL. The mixture was vigorously stirred for 2 hours at room temperature. The reaction mixture was washed with water and the solvent was filtered through a phase separator paper. After removal of the solvents, the crude product was purified by silica gel column chromatography (hexane/AcOEt = 5/2), to give desired product as a pale yellow solid (25 mg, 25 %). ^{1}H NMR (400 MHz, DMSO-d_6) δ: 8.25 (d, 7.2 Hz, 1H), 7.54 (d, *J* = 7.6 Hz, 1H), 7.45–7.27 (m, 9H), 7.22–7.12 (m, 4H), 5.78–5.75 (m, 2H), 3.46–3.38 (m, 4H). ^{13}C NMR (400 MHz, $CDCl_3$) δ: 184.76, 149.37, 147.08, 146.86, 141.07, 139.61, 139.16, 134.09, 132.86, 130.83, 130.10, 129.61, 128.31, 128.13, 126.69, 126.65, 126.35, 125.30, 123.01, 122.43, 120.73, 120.21, 118.03, 63.15, 31.08, 30.63. HRMS (ESI-TOF) calculated for $C_{33}H_{22}N_2O$ $[M+H]^+$: 463.11804, found: 463.1826.

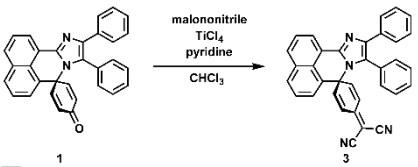

Scheme 4. Synthetic Scheme of **3**.

*Np-PIC (**1**)* was prepared according to a literature procedure.[26]

*Compound **3**.* 0.1 mL (0.1 mmol) of thionyl chloride (1 M in CH_2Cl_2) was added into a solution of **1** (10 mg, 0.023 mmol), malononitrile (9 mg, 0.14 mmol) and anhydrous pyridine (0.010 mL, 0.14 mmol) in 2.0 mL of anhydrous $CHCl_3$ at 0 °C under N_2 atmosphere. The mixture is refluxed at 60 °C for 2 days. After the quenching with water, the reaction mixture was extracted with CH_2Cl_2. The organic extract was washed with water and brine, and filtered through a phase separator paper. After removal of the solvents, the crude product was purified by silica gel column chromatography (AcOEt/hexane = 1/3), to give desired product as a orange solid (7.0 mg, 63 %). ^{1}H NMR (400 MHz, DMSO-d_6) δ: 8.44 (d, *J* = 6.4 Hz, 1H), 8.07 (t, *J* = 8.4 Hz, 2H), 7.78 (t, *J* = 7.2 Hz, 1H), 7.58–7.36 (m,8H), 7.24–7.08 (m, 6H), 6.46 (d, *J* = 9.6 Hz, 2H). ^{13}C NMR (400 MHz, $CDCl_3$) δ: 153.89, 145.77, 140.78, 133.46, 132.93, 130.80, 129.76, 129.22, 128.74, 128.59, 128.21, 127.41, 126.93, 126.69, 126.25, 126.16, 126.17, 124.01, 121.67, 121.53, 119.74, 111.69, 82.09, 63.12. HRMS (ESI-TOF) calculated for $C_{34}H_{20}N_4$ $[M+H]^+$: 485.1761, found: 485.1747.

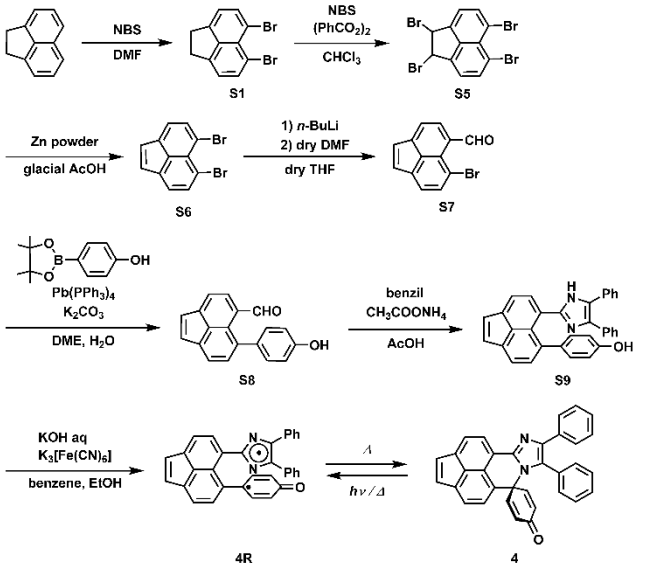

Scheme 5. Synthetic Scheme of **4**.

*1,2,5,6-Tetrabromo-1,2-dihydroacenaphthylene (**S5**)* and *5,6-dibromoacenaphthylene (**S6**)* were prepared according to a literature procedure.[36]

*6-Bromoacenaphthylene-5-carbaldehyde (**S7**).* 0.75 mL (1.2 mmol) of *n*-butyl lithium solution (1.55 M in hexane) was added into a solution of 300 mg (0.967 mmol) of 5,6-dibromoacenaphthylene (**S6**) in 3 mL of anhydrous THF at −78 °C under N_2 atmosphere. The resulting reaction mixture was stirred at −78 °C for 20 minutes, treated with 0.60 mL (7.7 mmol) of anhydrous DMF, and then kept stirred at −78 °C for 50 minutes. The reaction mixture was slowly warmed to room temperature, and stirred for 30 minutes at room temperature. After the quenching with water, the reaction mixture was extracted with CH_2Cl_2. The organic extract was washed with water and brine, and filtered through a phase separator paper. After removal of the solvents, the crude product was purified by silica gel column chromatography (AcOEt/hexane = 1/10), to give desired product as a yellow solid (189.6 mg, 76 %). ^{1}H NMR (400 MHz, $CDCl_3$) δ: 11.61 (s, 1H), 8.12 (d, *J* = 6.8 Hz, 1H), 7.87 (7.2 Hz, 1H), 7.73 (d, *J* = 7.2 Hz, 1H), 7.47 (d, *J* = 7.2 Hz, 1H), 7.10 (d, *J* = 5.2 Hz, 1H), 6.98 (d, *J* = 5.6 Hz, 1H).

*6-(4-Hydroxyphenyl)acenaphthylene-5-carbaldehyde (**S8**).* K_2CO_3 (71 mg, 0.52 mmol), 6-bromoacenaphthylene-5-carbaldehyde (**S6**) (190 mg, 0.732 mmol), and 4-(4,4,5,5-tetramethyl-1,3,2-dioxaborolan-2-yl)phenol (195 mg, 0.887 mmol) were added to DME (6.0 mL) and water (2.0 mL) and the mixture was purged with N_2 gas. $Pd(PPh_3)_4$ (23 mg, 0.020 mmol) was added to the solution and the solution was refluxed for 6 hours. The reaction mixture was extracted with CH_2Cl_2, and the organic extract was washed with water and brine, and filtered through a phase separator paper. After removal of the solvents, the crude product was purified by silica gel column chromatography (CH_2Cl_2/AcOEt = 15/1), to give desired product as a orange solid (161 mg, 81 %). ^{1}H NMR (400 MHz, DMSO-d_6) δ: 9.81 (br, 1H), 9.42 (s, 1H), 8.03 (d, *J* = 7.2 Hz, 1H), 7.96 (d, *J* = 7.2 Hz, 1H), 7.88 (d, *J* = 6.8 Hz, 1H), 7.56 (d, *J* = 7.2 Hz, 1H), 7.37 (d, *J* = 5.2 Hz, 1H), 7.25 (d, *J* = 8.4 Hz, 2H), 7.22 (d, *J* = 5.2 Hz, 1H), 6.92 (d, *J* = 8.4 Hz, 2H).

*4-(6-(4,5-Diphenyl-1H-imidazol-2-yl)acenaphthylen-5-yl)phenol (**S9**).* 6-(4-hydroxyphenyl)acenaphthylene-5-carbaldehyde (**S8**) (161 mg, 0.592 mmol), benzil (229 mg, 1.09 mmol) and ammonium acetate (586 mg, 7.60 mmol) were dissolved in acetic acid 7.5 mL. The mixture was stirred at 110 °C for 11 hours. After cooling to room temperature, the reaction mixture was neutralized with aqueous NH_3, and the aqueous layer was extracted with AcOEt. The combined organic layer was washed with water and brine, filtered through a phase separator paper, and evaporated. After removal of the solvents, the crude product was purified by silica gel column chromatography (CH_2Cl_2/AcOEt = 2/1), to give desired product as a yellow solid (102 mg, 37 %). ^{1}H NMR (400 MHz, DMSO-d_6) δ: 11.75 (s, 1H), 9.14 (s, 1H), 7.90 (d, *J* = 6.8 Hz, 1H), 7.84 (d, *J* = 7.2 Hz, 1H), 7.80 (d, *J* = 7.2 Hz, 1H), 7.46 (d, *J* = 6.8 Hz, 1H), 7.39 (d, *J* = 8.4 Hz, 2H), 7.31–7.13 (m, 10H), 7.02 (d, *J* = 8.0 Hz, 2H), 6.46 (d, *J* = 8.8 Hz, 1H).

*Compound **4**.* To a solution of 4-(6-(4,5-diphenyl-1*H*-imidazol-2-yl)acenaphthylen-5-yl)phenol (**S9**) (5 mg, 0.011 mmol) in benzene 2 mL and ethanol 0.02 mL was added KOH (82 mg, 1.5 mmol) and $K_3[Fe(CN)_6]$ (48 g, 0.15 mmol) in water 2 mL. The mixture was vigorously stirred for 2 hours at room temperature. The reaction mixture was washed with water and the solvent was filtered through a phase separator paper. After removal of the solvents, the crude product was purified by silica gel column chromatography (CH_2Cl_2/AcOEt = 60/1), to give desired product as an orange solid (1 mg, 20 %). ^{1}H NMR (400 MHz, DMSO-d_6) δ: 8.30 (d, *J* = 7.2 Hz, 1H), 8.02 (d, *J* = 7.2 Hz, 1H), 7.84 (d, *J* = 7.6 Hz, 1H), 7.47–7.18 (m, 15H), 5.91 (d, *J* = 10.0 Hz, 1H). ^{13}C NMR (400 MHz, $CDCl_3$) δ: 183.52, 147.57, 138.69, 138.27, 132.79, 131.81, 129.86, 129.76, 129.67, 129.47, 129.25, 128.31, 127.31, 127.23, 127.17, 126.93, 126.47, 125.87, 125.64, 124.68, 123.43, 121.62, 120.41, 118.95. HRMS (ESI-TOF) calculated for $C_{33}H_{20}N_2O$ $[M+H]^+$: 461.1648, found: 461.1650.

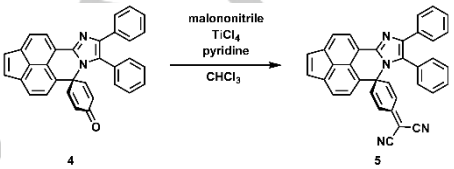

Scheme 6. Synthetic Scheme of **5**.

*Compound **5**.* 0.5 mL (0.5 mmol) of thionyl chloride (1 M in CH_2Cl_2) was added into a solution of compound 4 (47 mg, 0.10 mmol), malononitrile (39 mg, 0.59 mmol) and anhydrous pyridine (0.050 mL, 0.62 mmol) in 3.4 mL of anhydrous $CHCl_3$ at 0 °C under N_2 atmosphere. The mixture is refluxed at 60 °C for 26 hours. After the quenching with water, the reaction mixture was extracted with CH_2Cl_2. The organic extract was washed with water and brine, and filtered through a phase separator paper. After removal of the solvents, the crude product was purified by silica gel column chromatography (AcOEt/hexane = 1/4), to give desired product as an orange solid (28 mg, 54 %). ^{1}H NMR (400 MHz, DMSO-d_6) δ: 8.30 (d, *J* = 7.2 Hz, 1H), 8.02 (d, *J* = 7.2 Hz, 1H), 7.81 (d, *J* = 7.2 Hz, 1H), 7.52–7.49 (m, 1H), 7.47 (d, *J* = 7.2 Hz, 2H), 7.40 (d, *J* = 4.4 Hz, 4H), 7.27–7.14 (m, 6H), 7.04 (d, *J* = 9.6 Hz, 2H), 6.54 (d, *J* = 9.6 Hz, 2H). ^{13}C NMR (400 MHz, $CDCl_3$) δ: 153.89, 145.77, 140.78, 133.75, 132.93, 130.80, 129.76, 129.22, 128.74, 128.59, 128.21, 127.41, 126.93, 126.69, 126.25, 125.17, 124.01, 121.67, 121.53, 119.74, 111.69, 82.09, 63.12. HRMS (ESI-TOF) calculated for $C_{36}H_{20}N_4$ $[M+H]^+$: 509.1760, found: 509.1767.

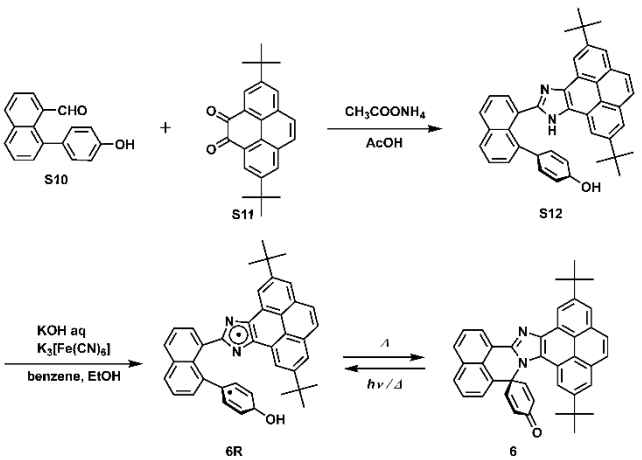

Scheme 7. Synthetic Scheme of **6**.

*8-(4-Hydroxyphenyl)-1-naphthaldehyde (**S10**)* was prepared according to a literature procedure.[26]

*2,7-di-tert-butylpyrene-4,5-dione (**S11**)* was prepared according to a literature procedure.[37]

*(1s,4s)-4-(8-(2,7-di-tert-butyl-9H-pyreno[4,5-d]imidazol-10-yl)naphthalen-1-yl)cyclohexa-2,5-dien-1-ol (**S12**).* 8-(4-hydroxyphenyl)-1-naphthaldehyde (**S11**) (25 mg, 0.10 mmol), 2,7-di-*tert*-butylpyrene-4,5-dione (40 mg, 0.12 mmol) and ammonium acetate (60 mg, 0.78 mmol) were dissolved in acetic acid 1 mL. The mixture was stirred at 110 °C for 17 hours. After cooling to room temperature, the reaction mixture was neutralized with aqueous NH_3, and the aqueous layer was extracted with AcOEt. The combined organic layer was washed with water and brine, filtered through a phase separator paper, and evaporated. After removal of the solvents, the crude product was purified by silica gel column chromatography (CH_2Cl_2/AcOEt = 10/1), to give desired product as a pale yellow solid (43 mg, 75 %). ^{1}H NMR (400 MHz, $CDCl_3$) δ: 8.97 (s, 1H), 8.86 (d, *J* = 1.6 Hz, 1H), 8.23 (d, *J* = 6.8 Hz, 1H), 8.08–7.95 (m, 6 H), 7.76 (s, 1H), 7.66 (dd, *J* = 7.2, 11.2 Hz, 2H), 7.57 (d, 0.8 Hz, 1H), 7.10 (d, 7.6 Hz, 2H), 6.12 (d, 8.0 Hz, 2H), 4.79 (s, 1H), 1.59 (s, 1H), 1.55(s, 1H).

*Compound **6**.* To a solution of (1s,4s)-4-(6-(2,7-di-*tert*-butyl-9*H*-pyreno[4,5-d]imidazol-10-yl)acenaphthylen-5-yl)cyclohexa-2,5-dien-1-ol (**S11**) (20 mg, 0.035 mmol) in benzene 12 mL was added KOH (170 mg, 3.03 mmol) and $K_3[Fe(CN)_6]$ (793 mg, 2.41 mmol) in water 20 mL. The mixture was vigorously stirred for 2 hours at room temperature. The reaction mixture was washed with water and the solvent was filtered through a phase separator paper. After removal of the solvents, the crude product was purified by silica gel column chromatography (CH_2Cl_2/AcOEt = 1/1), to give desired product as an orange solid (6 mg, 30 %). ^{1}H NMR (400 MHz, $CDCl_3$) δ: 9.17 (d, *J* = 6.4 Hz, 1H), 8.96 (dd, *J* = 0.8, 7.2 Hz, 1H), 8.53 (d, 2.0, 1H), 8.20 (s,1H), 8.19 (s, 1H), 8.12 (dd, *J* = 0.8, 6.8 Hz, 2H), 7.93 (d, *J* = 0.8 Hz, 1H), 7.91 (d, *J* =0.8 Hz, 1H), 7.72 (t, 7.2 Hz, 1H), 7.68–7.57 (m, 2H), 7.54–7.50 (m, 2H), 1.67 (s, 1H), 1.49(s, 1H). ^{13}C NMR (400 MHz, $CDCl_3$) δ: 152.74, 149.27, 148.21, 144.81, 141.27, 132.94, 131.66, 131.22, 129.29, 129.14, 128.46, 128.34, 128.08, 127.63, 127.56, 127.48, 126.48, 125.95, 125.74, 124.81, 123.30, 122.08, 121.98, 121.94, 121.87, 121.80, 121.35, 119.85, 1175.05. HRMS (ESI-TOF) calculated for $C_{41}H_{34}N_2O$ [M+H]$^+$: 571.2743, found: 571.2743.

Acknowledgements

This work was supported by JSPS KAKENHI Grant Number JP18H05263. This work was also supported by Aoyama Gakuin University Research Institute “Early Eagle” grant program for promotion of research by early career researchers.

Keywords: photochromism • visible light • biradical • imidazole

[1] M. Irie, T. Fukaminato, K. Matsuda, S. Kobatake, *Chem. Rev.* **2014**, *114*, 12174-12277.
[2] V. Balzani, A. Credi, F. M. Raymo, J. F. Stoddart, *Angew. Chem., Int. Ed.* **2000**, *39*, 3348-3391.
[3] *Molecular Switches* (Eds.: B. L. Feringa, W. R. Browne), Wiley-VCH, Weinheim, **2011**.
[4] *Photon-Working Switches* (Eds.: Y. Yokoyama, K. Nakatani), Springer: Tokyo, **2017**.
[5] I. Shimizu, H. Kokado, E. Inoue, *Bull. Chem. Soc. Jpn.* **1969**, *42*, 1730-1734.
[6] J. Sunamoto, K. Iwamoto, M. Akutagawa, M. Nagase, H. Kondo, *J. Am. Chem. Soc.* **1982**, *104*, 4904-4907.
[7] F. Ciardelli, D. Fabbri, O. Pieroni, A. Fissi, *J. Am. Chem. Soc.* **1989**, *111*, 3470-3472.
[8] M. Tanaka, M. Nakamura, M. A. A. Salhin, T. Ikeda, K. Kamada, H. Ando, Y. Shibutani, K. Kimura, *J. Org. Chem.* **2001**, *66*, 1533-1537.
[9] H.-R. Blattmann, D. Meuche, E. Heilbronner, R. J. Molyneux, V. Boekelheide, *J. Am. Chem. Soc.* **1965**, *87*, 130-131.
[10] R. H. Mitchell, *Eur. J. Org. Chem.* **1999**, 2695-2703.
[11] K. Honda, H. Komizu, M. Kawasaki, *J. Chem. Soc., Chem. Commun.* **1982**, 253-254.
[12] S. Helmy, F. A. Leibfarth, S. Oh, J. E. Poelma, C. J. Hawker, J. Read de Alaniz, *J. Am. Chem. Soc.* **2014**, *136*, 8169-8172.
[13] J. R. Hemmer, S. O. Poelma, N. Treat, Z. A. Page, N. D. Dolinski, Y. J. Diaz, W. Tomlinson, K. D. Clark, J. P. Hooper, C. Hawker, J. Read De Alaniz, *J. Am. Chem. Soc.* **2016**, *138*, 13960-13966.
[14] J. R. Hemmer, Z. A. Page, K. D. Clark, F. Stricker, N. D. Dolinski, C. J. Hawker, J. Read De Alaniz, *J. Am. Chem. Soc.* **2018**, *140*, 10425-10429.
[15] J. C. Crano, R. J. Guglielmetti, *Organic Photochromic and Thermochromic Compounds*, Plenum Press, New York, **1999**.
[16] H. Kuroiwa, Y. Inagaki, K. Mutoh, J. Abe, *Adv. Mater.* **2019**, *31*, 1805661.
[17] E. Deniz, M. Tomasulo, J. Cusido, S. Sortino, F. M. Raymo, *Langmuir* **2011**, *27*, 11773-11783.
[18] K. Mutoh, M. Sliwa, J. Abe, *J. Phys. Chem. C* **2013**, *117*, 4808-4814.
[19] N. Ishii. T. Kato, J. Abe, *Sci. Rep.* **2012**, *2*, 819.
[20] Y. Kobayashi, J. Abe, *Adv. Optical Mater.* **2016**, *4*, 1354-1357.
[21] S. Hatano, T. Horino, A. Tokita, T. Oshima, J. Abe, *J. Am. Chem. Soc.* **2013**, *135*, 3164-3172.
[22] I. Yonekawa, K. Mutoh, Y. Kobayashi, J. Abe, *J. Am. Chem. Soc.* **2018**, *140*, 1091-1097.
[23] I. Yonekawa, K. Mutoh, J. Abe, *Chem. Commun.* **2019**, *55*, 1221-1224.
[24] K. Mutoh, N. Miyashita, K. Arai, J. Abe, *J. Am. Chem. Soc.* **2019**, *141*, 5650-5654.
[25] T. Yamaguchi, Y. Kobayashi, J. Abe, *J. Am. Chem. Soc.* **2016**, *138*, 906-913.
[26] K. Mutoh, Y. Kobayashi, Y. Hirao, T. Kubo, J. Abe, *Chem. Commun.* **2016**, *52*, 6797-6800.
[27] Y. Satoh, Y. Ishibashi, S. Ito, Y. Nagasawa, H. Miyasaka, H. Chosrowjan, S. Taniguchi, N. Mataga, D. Kato, A. Kikuchi, J. Abe, *Chem. Phys. Lett.* **2007**, *448*, 228-231.
[28] H. Miyasaka, Y. Satoh, Y. Ishibashi, S. Ito, S. Taniguchi, H. Chosrowjan, N. Mataga, D. Kato, A. Kikuchi, J. Abe, *J. Am. Chem. Soc.* **2009**, *131*, 7256-7263.
[29] K. Mutoh, E. Nakano, J. Abe, *J. Phys. Chem. A* **2012**, *116*, 6792-6797.
[30] K. Yamamoto, K. Mutoh, J. Abe, *J. Phys. Chem. A* **2019**, *123*, 1945-1952.
[31] E. Nakano, K. Mutoh, Y. Kobayashi, J. Abe, *J. Phys. Chem. A* **2014**, *118*, 2288-2297.
[32] K. Yamamoto, I. Gomita, H. Okajima, A. Sakamoto, K. Mutoh, J. Abe, *Chem. Commun*. **2019**, *55*, 4917-4920.
[33] F. A. Carey, R. J. Sundberg, *Advanced Organic Chemistry: Part A: Structure and Mechanisms*, Springer, **2007**.
[34] T. Nakagawa, K. Okamoto, H. Hanada, R. Katoh, *Opt. Lett.* **2016**, *41*, 1498-1501.
[35] M. A. Niyas, R. Ramakrishnan, V. Vijay, E. Sebastian, M. Hariharan, *J. Am. Chem. Soc.* **2019**, *141*, 4536-4540.
[36] L. M. Diamond, F. R. Knight, K. S. A. Arachchige, R. A. M. Randall, M. Bühl, A. M. Z. Slawin, J. D. Woollins, *Eur. J. Inorg. Chem.* **2014**, *9,* 1512-1523.
[37] P.-Y. Gu, Z. Wang, G. Liu, H. Yao, Z. Wang, Y. Li, J. Zhu, S. Li, Q. Zhang, *Chem. Mater.* **2017**, *29*, 4172-4175.

10.1002/cphc.202000296

WILEY-VCH

ARTICLE

Entry for the Table of Contents

Insert graphic for Table of Contents here.

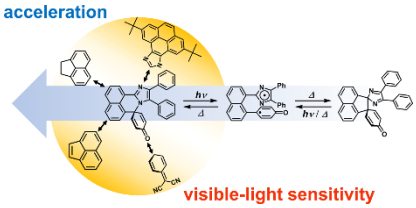

A fast switchable negative photochromic molecule is useful as a photo-switch aiming to the application to functional materials. Herein, we succeed in the control of the thermal back reaction rates and the enhancement of the visible-light sensitivity of the naphthalene-bridged phenoxyl-imidazolyl radical complex (Np-PIC). These insights will be important for the future development of fast switchable negative photochromic molecules.